NANO LETTERS

Letter

pubs.acs.org/NanoLett

Writing on Superhydrophobic Nanopost Arrays: Topographic Design for Bottom-up Assembly

Benjamin D. Hatton* and Joanna Aizenberg

School of Engineering and Applied Sciences, Harvard University, Cambridge, Massachusetts, United States

Supporting Information

ABSTRACT: A well-known property of superhydrophobic surfaces, such as an array of hydrophobic nanoposts, is to allow only limited surface contact of a liquid to the tips of the nanoposts. Herein we demonstrate that material deposition from solution, whether solid precipitation, surface adsorption or colloidal adhesion in static system, or dynamic "writing", can be limited to these specific areas of the surface when in this nonwetting state. As an example of solid precipitation, we show that nucleation of $CaCO_3$ results in the growth of small, uniform, amorphous deposits (which can merge and recrystallize) instead of disordered, large crystals due to the abundance of identical, small heterogeneous nucleation sites. The growth of amorphous $CaCO_3$ can be used to trap molecules from solution, as a potential application for controlled drug release. To demonstrate the localized surface adsorption, we show that chemical functionalization of the post tips can make them "sticky" for specific attachment of species (such as colloidal particles) from solution. The electrostatic charge and relative size ratio of the particle/post diameters control the attachment of particles to the post tips with great specificity. Dynamic conditions have also been shown for writing using droplets translated across the nonwetting surface at controlled speeds during deposition. These methods offer unprecedented control over the heterogeneous nucleation and localized growth of crystals from solution and avoid nonspecific adsorption. There is selective control of colloidal or molecular attachment to the nanopost tips, whereby the contact area, time of contact, and tip surface chemistry for reaction are all independently tunable parameters.

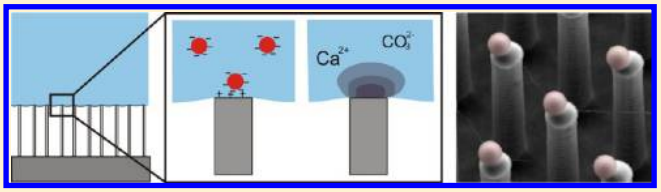

KEYWORDS: *Superhydrophobic, nucleation, calcium carbonate, precipitate, writing, colloidal patterning*

Control of the spatial position of material growth and deposition from solution on a surface remains one of the challenging aspects associated with bottom-up synthesis of structures at the nano- and microscale. A wide range of biological growth processes involve, however, highly evolved, specific nucleation events, such as those leading to biomineralization, antibody/antigen attachment, and protein interactions on tissue surfaces, when nonspecific adsorption or nucleation events are fully suppressed or prevented to control nanoscale details of the growing material. As a result, bionanocomposites, such as bone (collagen/hydroxyaptite) or mollusk shell (chitin/$CaCO_3$), are formed by a sequence of these nucleation events that determine a complex inorganic structure of well-defined size, spatial distribution, and crystallographic orientation.[1−3]

In contrast, there are limited synthetic approaches to define spatially where material should grow, or not grow, for bottom-up synthesis.[4,5] The patterning of precipitate or nanoparticles can be achieved by surface chemistry patterning, but typically with limited spatial resolution. For example, a 2D pattern of alkanethiol self-assembled monolayers can control the heterogeneous nucleation of $CaCO_3$ and other minerals,[6−9] patterned catalytic sites can control the nucleation and growth of nanowires and carbon nanotubes,[10−13] and electrostatic surface charge can direct colloids or nanowires.[14−16] However, in all cases the nonspecific adsorption and nucleation can be difficult to avoid, which limits the fidelity and spatial resolution, and the

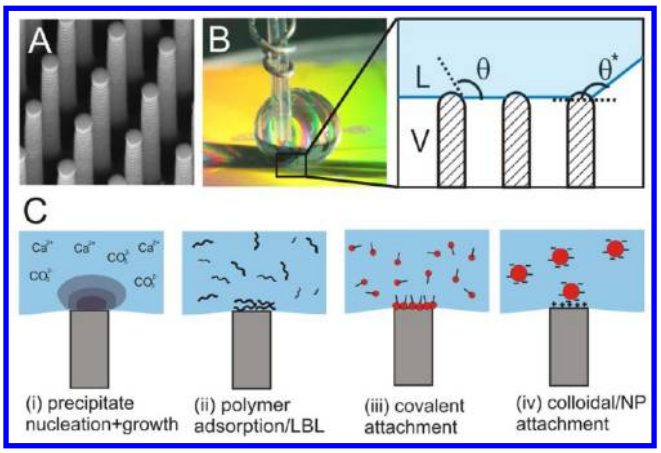

Figure 1. Mechanism of tip deposition. (A) SEM image of a Si post array, 1.5 μm diameter posts; (B) water droplet on the superhydrophobic post surface, showing (schematic) the position of the air−liquid interface for the Cassie state; (C) mechanisms of localized tip deposition from solution.

Received: May 11, 2012
Revised: July 27, 2012

   dx.doi.org/10.1021/nl301775x | *Nano Lett.* XXXX, XXX, XXX−XXX

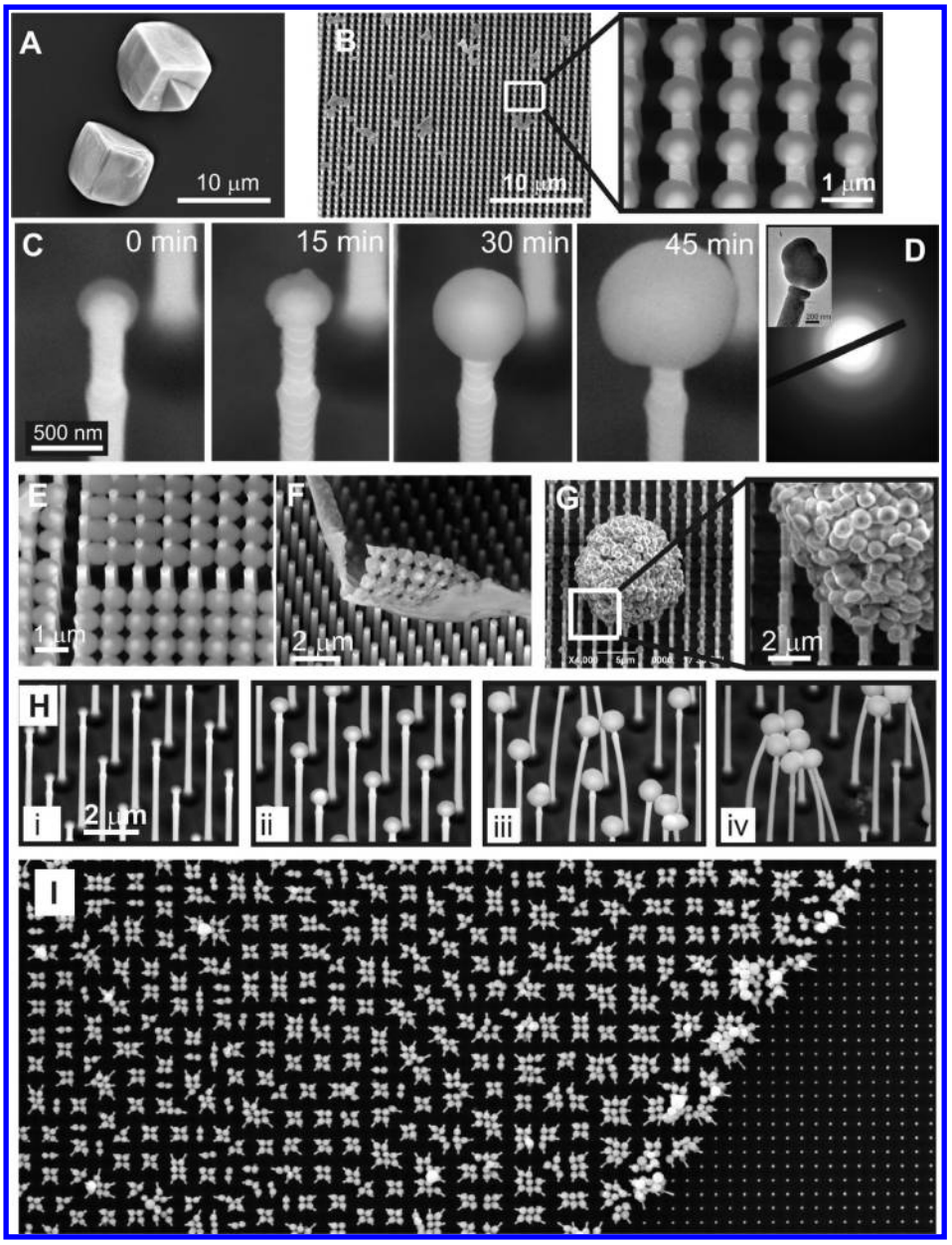

Figure 2. $CaCO_3$ deposition on post tips. (A) $CaCO_3$ growth (25 mM, 20 min) on a flat surface as calcite; (B) $CaCO_3$ growth (25 mM, 20 min) on an array of 300 nm diameter posts; (C) comparison of $CaCO_3$ growth as a function of time; (D) TEM image of a single $CaCO_3$ deposit; (E,F) growth of $CaCO_3$ spheres impinging upon each other as a sheet; (G) agglomerated $CaCO_3$ deposits, accumulated on the surface after detachment; (H) clustering behavior of $CaCO_3$ posts as a function of $CaCO_3$ growth; (I) clustering behavior over large areas at the edge of droplet perimeter.

conditions for each method can be highly specific to that system.

Herein we present a method for patterned deposition using the topography of a superhydrophobic surface, such as an array of posts (Figure 1A). Superhydrophobic surfaces combine a large roughness with a hydrophobic surface chemistry (i.e., contact angle $\theta > 90°$). As a result, it can be energetically favorable for the liquid to be spatially restricted to the tips of the surface features, in the so-called Cassie state, and cause an apparent contact angle (θ^*) larger than ~150° (Figure 1B).[17−19] Common biological examples include various plant leaves, insect cuticle and bird feathers,[20] while synthetic examples include arrays of micro- or nanoscale posts or nanoparticles.[21−23] Herein we demonstrate that because the liquid interface is limited to the tips of the surface features, any material deposition from solution, be it (i) precipitate nucleation and growth, (ii) physical or chemical adsorption (including layer-by-layer (LBL)), (iii) covalent surface reaction, or (iv) colloidal or nanoparticle attachment, can occur only on those points of the surface exposed to the liquid phase (Figure 1C). As a result, parameters that can influence a given deposition process (whether precipitation, particle attachment, etc.) can be independently controlled in a relatively simple way. The contact time, dimensions of the contact points, total contact area, and surface chemistry can each be used to tune the deposition from solution, and we refer to this method as topography-induced precipitation (TIP). These principle points make the TIP method a new, general approach to controlling materials design and precise placement on a 2D surface through the topography of the underlying substrate.

dx.doi.org/10.1021/nl301775x | *Nano Lett.* XXXX, XXX, XXX−XXX

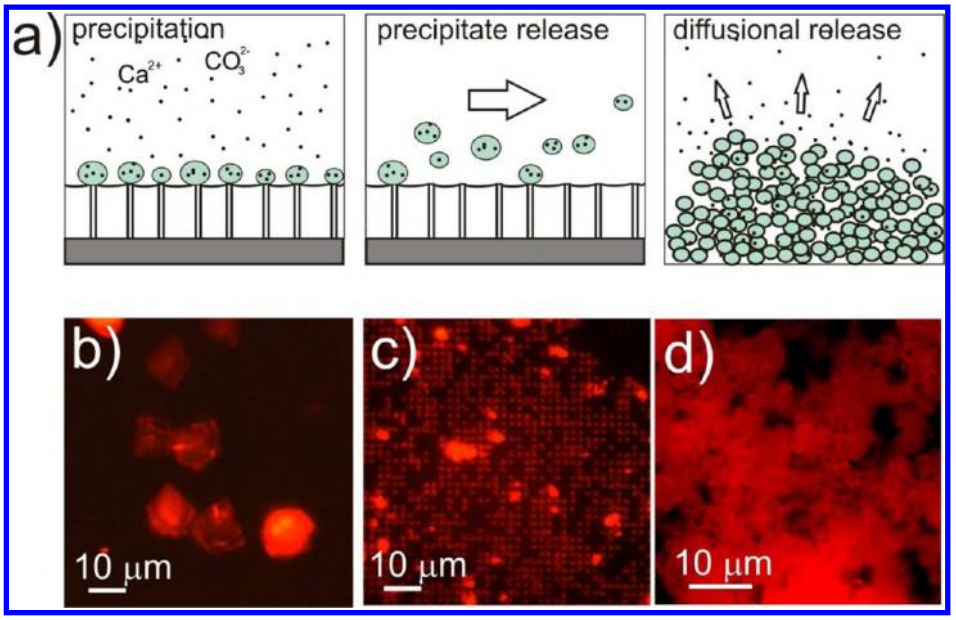

Figure 3. $CaCO_3$ deposition for molecular capture and release. (a) Schematic showing how the precipitation of $CaCO_3$ TIP particles in the presence of some dissolved species can be used for capture within the hydrated solid. Release and collection of the TIP particles could be used for diffusional release after $CaCO_3$ dissolution; $CaCO_3$ growth (50 mM, 30 min) in the presence of Rhodamine B dye (5 mM), (b) large calcite crystals grown on flat Si; (c) array of small amorphous $CaCO_3$ TIP particles on an array of 300 nm diameter Si posts; (d) aggregate of $CaCO_3$ TIP particles.

Experiment. Si (100) wafers were etched with post arrays by a deep reactive ion etching (DRIE) Bosch process,[24] where the post diameters ranged from 0.3 to 1.5 μm, with pitch spacing 2 to 4 μm and height 4 to 8 μm. A hydrophobic surface was generated by oxygen plasma cleaning (Diener Femto) and an overnight exposure in a vacuum chamber containing (heptadecafluoro-1,1,2,2-tetrahydrodecyl)-trichlorosilane (Gelest, 99%).

For $CaCO_3$ deposition, 40 μL droplets of $CaCl_2$ solutions (Aldrich, 5 − 100 mM) were deposited onto the superhydrophobic substrate in a closed glass desiccator containing 10 g of $(NH_4)_2CO_3$ powder (Aldrich). The $(NH_4)_2CO_3$ spontaneously decomposes to CO_2, H_2O, and NH_3 that diffuse into the $CaCl_2$ solution to cause precipitation of $CaCO_3$.[7]

For polymer deposition, a solution of polyvinyl alcohol (PVA) was prepared by dissolving 4.0 g of PVA (Fluka 6−98, $M_w \sim 47\,000$) in 200 mL of DI H_2O at 80 °C. A small amount of Rhodamine B dye (Fluka) was added for fluorescence imaging.

The 300 nm poly(methyl methacrylate) (PMMA) spheres were synthesized following a published procedure.[25] Red fluorescent (Rhodamine), COOH-terminated, 1.3 μm polystyrene (PS) spheres (ThermoScientific), and Au nanoparticles (50 nm, COOH-terminated, Ted Pella) were purchased and used as received.

Scanning electron microscopy (SEM) was performed (JEOL 6390, Zeiss Ultra 55) on the substrates without Au coating. Samples were prepared for transmission electron microscopy (TEM) (JEOL 2100) by scraping posts from the substrate using a razor blade and depositing onto a C-coated 400 mesh Cu grid (EMS) for imaging at 200 kV. Fluorescence optical imaging was performed with a Leica DMRX microscope.

Results and Discussion. As illustrated in Figure 1C, we investigated the effects of superhydrophobic nonwetting contact and tip geometry for the following several types of materials deposition: (1) precipitation of $CaCO_3$, (2) physical adsorption of polyvinyl alcohol (PVA) solution, and (3) colloidal particle attachment.

$CaCO_3$ Precipitation. Figure 1C(i) illustrates the exposed post tips acting as sites for heterogeneous nucleation, reducing the energy associated with precipitate formation. On a flat, hydrophobic Si surface (from here on referred to as Si−F), $CaCO_3$ grown from a 25 mM $CaCl_2$ solution for 20 min typically forms a disordered array of large (5−50 μm) crystals, which are mostly calcite rhombohedra (Figure 2A). Under the same growth conditions, $CaCO_3$ grown on an array of posts (300 nm diameter, 1 μm pitch) formed as a highly uniform distribution of spheres on each post tip (Figure 2B). The extent of growth is highly controllable (Figure 2C) as a function of the growth time (50 mM $CaCl_2$). In fact, for a fixed growth time (30 min), $CaCO_3$ deposit size was found to be relatively independent of the $CaCl_2$ concentration but did decrease gradually with the $CaCl_2$ solution droplet size and was highly dependent on the post density (for post arrays having roughly the same projected area, about 0.2), as shown in Supporting Information Figure S01. These observations suggest that the $CaCO_3$ growth rate is limited by the rate of CO_2 diffusion into the droplet (droplet size effect), while the diameter of $CaCO_3$ deposits is very much defined by the available nucleation sites; a large number of small posts produces smaller deposits than a small number of large posts.

Figure 2D is a TEM image of a single post (50 mM $CaCl_2$, 30 min) showing a lack of crystalline morphology, and the diffuse rings of the selected area electron diffraction (SAED) pattern indicate an atomic structure that is amorphous, or at least, nanocrystalline. Similar micrometer-scale spherical deposits of amorphous $CaCO_3$ can be formed through rapid growth kinetics, such as a rapid release of carbonate in solution.[26] But the controlled growth of uniform amorphous particles on a surface through a control of heterogeneous nucleation sites has never been demonstrated before.

It has been suggested and demonstrated experimentally that amorphous calcium carbonate (ACC) can be stable against

dx.doi.org/10.1021/nl301775x | *Nano Lett.* XXXX, XXX, XXX−XXX

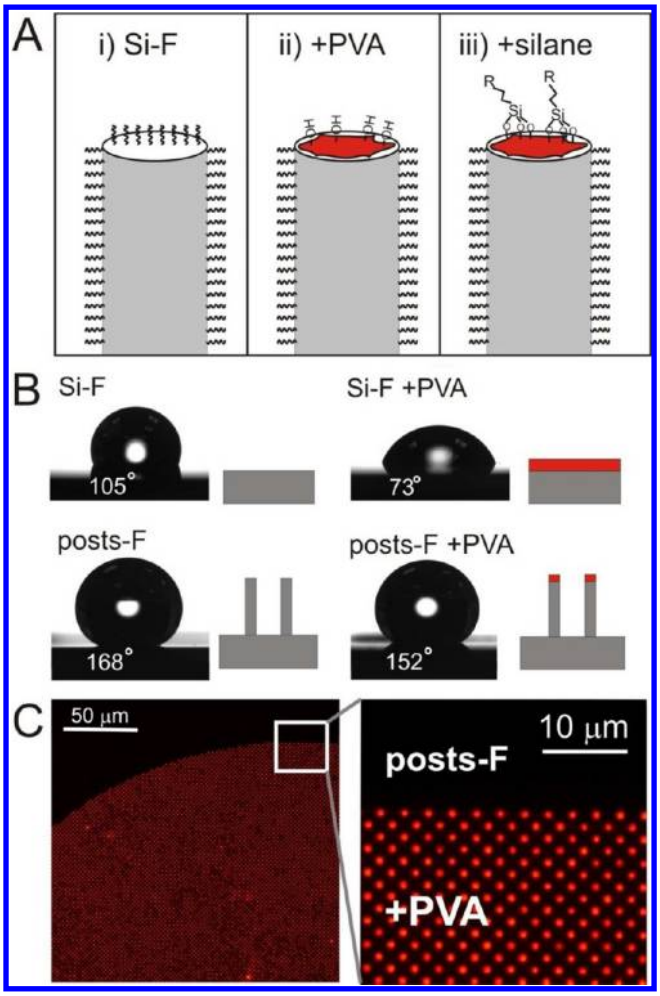

Figure 4. Tip functionalization. (A) Schematic of (i) fluorosilane-covered post (hydrophobic), (ii) after contact with PVA solution (hydrophilic tip), (iii) after contact with a silane vapor, such as APTES, to introduce functional groups; (B) contact angle results for flat hydrophobic Si (fluorosilane, Si−F), Si−F after contact with PVA solution (Si−F + PVA), hydrophobic Si post array (posts-F), and posts-F after contact with PVA solution (posts-F + PVA); (C) optical fluorescence image showing the fluorescent footprint of the rhodamine-PVA post tips after droplet contact.

recrystallization for small particle size ranges.[27,28] For example, it was found that 100 nm is the approximate threshold size limit to maintain the amorphous phase against crystallization.[29] Herein we have seen that these ACC particles, much larger than 100 nm, are stable against recrystallization for an extended length of time. A reason for this stable amorphous state may be because the particles are rapidly removed from the aqueous phase (upon droplet removal), and are thereby dry relatively quickly and remain dry, which would greatly delay the kinetics for recrystallization.

For extended amount of growth, the $CaCO_3$ deposits can begin to impinge upon one another if the posts are spaced closely enough, and even form a continuous sheet of the impinging amorphous growths (Figure 2E, F). When the droplet of growth solution is moved along, or removed from the surface, the $CaCO_3$ deposits can become detached from the posts and form agglomerated structures by the surface tension of the air/water interface (Figure 2G). We suggest that such particles could be 'harvested' in a continuous flow environment by a growth and size-dependent detachment process that would provide a way of making uniform colloidal particles of controlled size (Supporting Information Figure S02). Alternatively the posts can become "glued" together into clusters, depending on the deposit growth size (Figure 2H). Figure 2I shows interesting clustering patterns for an array of posts at the edge of the $CaCl_2$ droplet contact. With the size of $CaCO_3$ deposits increasing (for a fixed post spacing), there is a smaller distance for neighboring posts to touch, and a larger deposit contact area to glue. For some time, there has been a great interest in the controlled synthesis of amorphous $CaCO_3$ particles that can be shaped by a template intermediary and then recrystallized as a mimic of biogenic process for complex inorganic structures.[3,7,29] These results suggest that under controlled conditions the agglomerated structures of Figure 2 could be recrystallized as complex-shaped single or polycrystals from these amorphous particles.

An interesting application for this nucleation of monodispersed amorphous $CaCO_3$ particles is for the trapping of dissolved molecular species from solution into the hydrated precipitates as they grow. $CaCO_3$ particles have been investigated before as vessels for drug capture and release, largely because of their very good biocompatibility and biodegradability.[30−32] Figure 3A shows schematically how biomolecular species could be incorporated into the growing $CaCO_3$ particles before release from the nanopost surface and release of the drug upon dissolution. Figure 3B shows large calcite crystals grown in the presence of fluorescent dye (Rhodamine B), presumably incorporated into the $CaCO_3$ structure itself. Figure 3C,D shows that the small (1 μm) amorphous $CaCO_3$ TIP particles also appear to incorporate the fluorescent dye on the 300 nm posts and aggregated due to release from the surface. The amorphous phase may present interesting potential for rapid dissolution, and the TIP growth method allows for control of the particle size. Future work will be done to test the dissolution and chemical release from such particles.

Polymer Adsorption. Polymer adsorption onto the post tips can be used as a method of chemically functionalizing the tips of the otherwise hydrophobic nanopost arrays but maintain its superhydrophobic properties. Polyvinyl alcohol (PVA) in aqueous solution has previously been found to strongly physisorb onto hydrophobic surfaces.[33] We have taken advantage of this property to "paint" hydrophilic patches on the post tips of a superhydrophobic post array having fluorosilane-treated surfaces (Figure 4A). Exposure of a flat fluorinated Si (Si−F) surface to a 1% PVA solution (Si−F + PVA) causes the water contact angle to decrease from 105 to 73° (Figure 4B). This physisorption to the fluorinated surface is surprisingly stable against desorption (no change in contact angle after 1 h sonication in DI water). Similar results were found for chitosan, poly(acrylic acid), and collagen solutions. Exposure of the same 1% PVA solution to a Si post array (300 nm diameter posts, 2 μm pitch) caused a reduction in the contact angle from 168 to 152° (Figure 4B), but water droplets remained in a nonwetting, Cassie state, as indicated by the high droplet mobility (despite an increase in contact angle hysteresis). When a droplet containing 1% PVA solution and Rhodamine B dye was placed on the Si post array surface (10 s) and removed, a very clear "footprint" of the fluorescent polymer was left behind (Figure 4C). This fluorescent microscopy imaging clearly shows a sharp boundary region of those posts with "painted" tips next to a region with no polymer deposition. A useful property of this hydrophilic paint,

dx.doi.org/10.1021/nl301775x | *Nano Lett.* XXXX, XXX, XXX−XXX

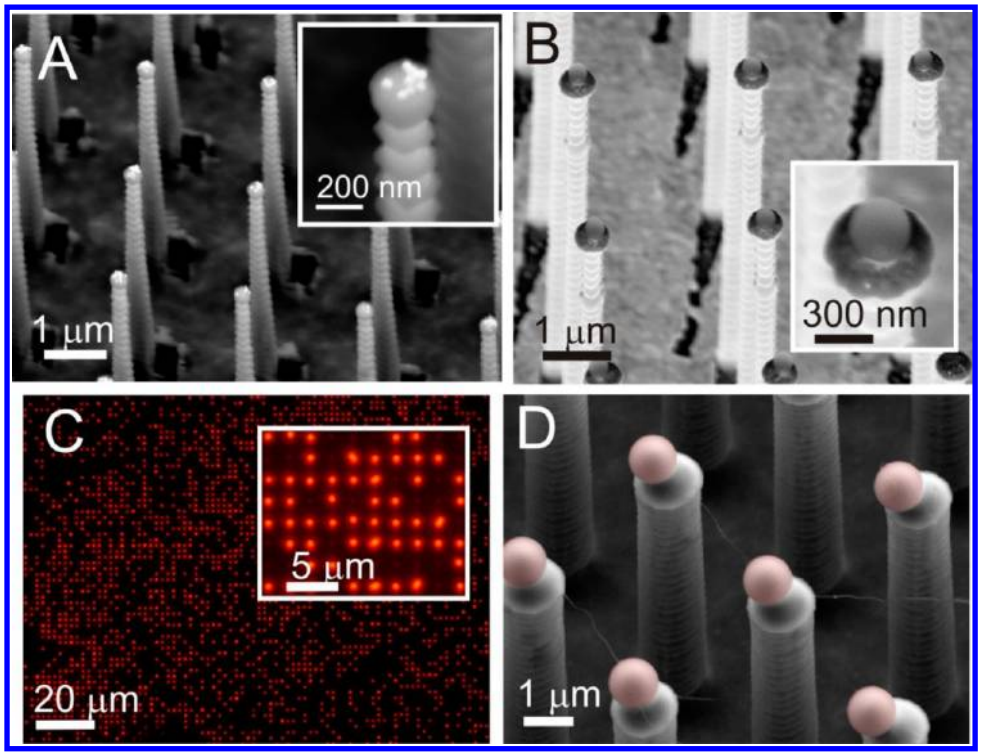

Figure 5. Particle deposition onto post tips functionalized with APTES. (A) The 50 nm Au nanoparticles on 300 nm Si posts; (B) 300 nm PMMA spheres (SO_4 terminated) on 300 nm Si posts; (C) fluorescence optical and (D) SEM images of fluorescent (Rhodamine B) 1.0 μm PS spheres on 1.5 μm Si posts (color added for contrast).

on the tip of each post, is to serve as a hydrated basal layer for additional functionalization by vapor silane deposition (i.e., 3-aminopropyltriethoxysilane, APTES), as shown schematically in Figure 4A. A consequence of these types of functionalization of the tips with a hydrophilic coating is that a dynamic, impacting droplet is still able to bounce from the nonwetting surface, but its kinetic energy is significantly reduced, presumably due to an increase in contact angle hysteresis and drag during dewetting (Supporting Information Figure S03).

Particle Attachment. The adhesion of colloidal particles to the post tips can be achieved by electrostatic charge attraction (Figure 1C(iv)). Figure 5A,B shows 50 nm negatively charged (COOH-terminated) Au nanoparticles and sulfate-terminated PMMA spheres (300 nm) attached to positively charged (amine-terminated) Si posts (300 nm diameter). Controlling the attachment of Au nanoparticles to tips of posts has important applications for new approaches to high-resolution spectroscopy (such as surface-enhanced Raman spectroscopy, SERS), as was recently shown for a superhydrophobic surface.[32] Finally, Figure 5C,D shows the deposition of negatively charged, red fluorescent 1.3 μm PS particles deposited onto amine-terminated posts, both in fluorescent imaging and SEM, respectively. Conversely, exposure of colloidal suspension to hydrophobic posts, or for similarly charged particles and posts, did not result in any significant colloidal deposition. Further, it was found that if the size ratios of particle to post diameter was too high (i.e., >1), then particle attachment was not observed, which may be caused by surface tension-based detachment upon removal of the (nonwetting) droplet of colloidal suspension from the surface.

Dynamic Writing. An interesting consequence of the mobile, nonwetting contact of a droplet on these superhydrophobic surfaces is that deposition can be achieved dynamically for a moving droplet (as shown in Figure 6A), leaving behind a printed (i.e., "written") trail of deposited polymer, precipitate or particles. As a result, patterns can be written on a 2D surface, as a kind of nonwetting ink droplet in an entirely new method of spatially defined surface deposition. Figure 6B shows a written trail of fluorescently labeled PVA polymer deposited onto the tips of 300 nm diameter, 2 μm pitch Si posts by sliding a 3 mm droplet at a rate of 1 mm/s (direction indicated by arrow). There exists a sharp boundary between the regions of the substrate in contact with the droplet and those that were not. A further demonstration is shown in Figure 6C for the deposition of $CaCO_3$ from a 100 mM $CaCl_2$ droplet slowly dragged across a 300 nm diameter, 2 μm pitch post array surface at 1 mm/min in a $(NH_4)_2CO_3$ environment to leave behind a trail of $CaCO_3$ deposits (direction indicated by arrow).

Summary. We have demonstrated an extremely fine control over a selective localized precipitation of organic and inorganic species, colloidal or molecular attachment to the post tips and dynamic "writing" on the exposed tips, where the contact area, time of contact, and tip surface chemistry for reaction are all independently controllable parameters. The limited surface contact of the superhydrophobic surface gives us unprecedented control over the heterogeneous nucleation and growth of precipitates from solution by providing identical nucleation sites and avoiding nonspecific adsorption. This TIP method represents an opportunity to "write" on the tips of a post array, where the post size and spacing and rate of droplet motion can determine the size, morphology and spatial distribution of the deposited material. Heterogeneous nucleation itself is a phenomenon that is not well understood, and, previously, there have been few experimental methods available to test, independently, the effects of nucleation site size, distribution,

dx.doi.org/10.1021/nl301775x | *Nano Lett.* XXXX, XXX, XXX−XXX

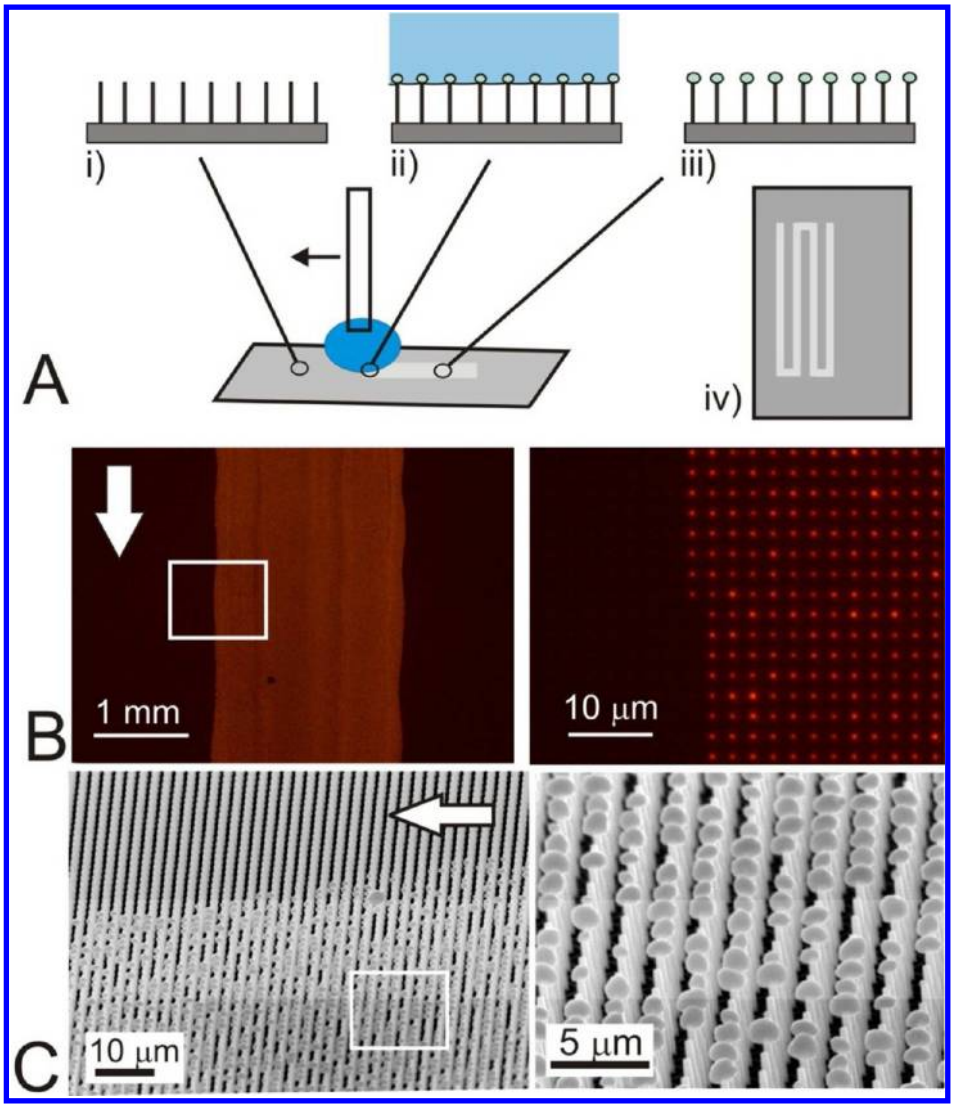

Figure 6. Dynamic writing on superhydrophobic surfaces. (A) Schematic of writing on a superhydrophobic post array surface, (i) before droplet contact, (ii) during growth, and (iii) in the trailing edge after growth. As a result, an arbitrary pattern can be written on the surface (iv). (B) Fluorescence images of a trail of Rhodamine-PVA written on 300 nm Si posts (arrow shows droplet direction, 1 mm/s); (C) SEM images of $CaCO_3$ TIP particles written on 300 nm Si posts (arrow shows droplet direction, 1 mm/min).

and chemistry on a surface. We have shown the deposition of identical, amorphous $CaCO_3$ spheres without additives to stabilize the amorphous phase and where the deposit size is highly dependent on the post size. This morphology is highly unusual and seems to be only possible when presented with such an array of identical, small, nucleation sites. This control of amorphous $CaCO_3$ formation may be useful for drug capture and controlled release as we have shown for fluorescent dye capture.

Further, we have demonstrated a method to chemically functionalize the post tips, which can be used to control particle attachment, spatially, with specificity for particle size and charge. Such functionalization could be used to further control the size, morphology, and crystallographic orientation of precipitate nuclei. This precise control of the nucleation site size and position presents a route toward the bottom-up engineering of selectively functionalized nanowires for a range of applications associated with solar photovoltaics, biochemical sensing, catalysis, or generating nanowire heterostructures.

■ ASSOCIATED CONTENT

Ⓢ Supporting Information

Figures S01−S03. This material is available free of charge via the Internet at http://pubs.acs.org.

■ AUTHOR INFORMATION

Corresponding Author

*E-mail: bhatton@seas.harvard.edu.

Notes

The authors declare no competing financial interest.

■ REFERENCES

(1) Mann, S.; Ozin, G. A. *Nature* **1996**, *382*, 313.
(2) Lowenstam, H. A.; Weiner, S. *On Biomineralization*; Oxford University Press: Oxford, 1989.
(3) Meldrum, F. C.; Cölfen, H. *Chem. Rev.* **2008**, *108*, 4332.
(4) Sanchez, C.; Arribart, H.; Guille, M. M. G. *Nat. Mater.* **2005**, *4*, 277.
(5) Woodson, M.; Liu, J. *Phys. Chem. Chem. Phys.* **2007**, *9*, 207.

dx.doi.org/10.1021/nl301775x | *Nano Lett.* XXXX, XXX, XXX−XXX

(6) Rieke, P. C.; Tarasevich, B. J.; Wood, L. L.; Engelhard, M. H.; Baer, D. R.; Fryxell, G. E.; John, C. M.; Laken, D. A.; Jaehnig, M. C. *Langmuir* **1994**, *10*, 619.
(7) Aizenberg, J.; Black, A. J.; Whitesides, G. M. *Nature* **1999**, *398*, 495.
(8) Meldrum, F. C.; Flath, J.; Knoll, W. *Thin Solid Films* **1999**, *348*, 188.
(9) Naka, K.; Chujo, Y. *Chem. Mater.* **2001**, *13*, 3245.
(10) Bennett, R. D.; Hart, A. J.; Miller, A. C.; Hammond, P. T.; Irvine, D. J.; Cohen, R. E. *Langmuir* **2006**, *22*, 8273.
(11) Hsu, J. W. P.; Tian, Z. R.; Simmons, N. C.; Matzke, C. M.; Voigt, J. A.; Liu, J. *Nano Lett.* **2005**, *5*, 83.
(12) Fuhrmann, B.; Leipner, H. S.; Hoche, H.-R.; Schubert, L.; Werner, P.; Gosele, U. *Nano Lett.* **2005**, *5*, 2524.
(13) Lu, J. Q.; Kopley, T. E.; Moll, N.; Roitman, D.; Chamberlin, D.; Fu, Q.; Liu, J.; Russell, T. P.; Rider, D. A.; Manners, I.; Winnik, M. A. *Chem. Mater.* **2005**, *17*, 2227.
(14) Velev, O. D.; Kaler, E. W. *Langmuir* **1999**, *15*, 3693.
(15) Aizenberg, J.; Braun, P. V.; Wiltzius, P. *Phys. Rev. Lett.* **2000**, *84*, 2997.
(16) Huang, J.; Tao, A. R.; Connor, S.; He, R.; Yang, P. *Nano Lett.* **2006**, *6*, 524.
(17) Cassie, A.; Baxter, S. *Trans. Faraday Soc.* **1944**, *40*, 546.
(18) Quere, D. *Ann. Rev. Mater. Res.* **2008**, *38*, 71.
(19) Callies, M.; Quere, D. *Soft Matter* **2005**, *1*, 55.
(20) Barthlott, W.; Neinhuis, C. *Planta* **1997**, *202*, 1.
(21) Feng, X.; Jiang, L. *Adv. Mater.* **2006**, *18*, 3063.
(22) Oner, D.; McCarthy, T. J. *Langmuir* **2000**, *16*, 7777.
(23) Guo, Z.; Liu, W.; Su, B. L. *J. Colloid Interface Sci.* **2011**, *353*, 335.
(24) Krupenkin, T. N.; Taylor, J. A.; Schneider, T. M.; Yang, S. *Langmuir* **2004**, *20*, 3824.
(25) Goodwin, J. W.; Hearn, J.; Ho, C. C.; Ottewill, R. H. *Colloid Polym. Sci.* **1973**, *252*, 464.
(26) Faatz, M.; Grohn, F.; Wegner, G. *Adv. Mater.* **2004**, *16*, 996.
(27) Navrotsky, A. *Proc. Natl. Acad. Sci. U.S.A.* **2004**, *101*, 12096.
(28) Nudelman, F.; Sonmezler, E.; Bomans, P. H. H.; Sommerdijk, N. A. J. M. *Nanoscale* **2010**, *2*, 2436.
(29) Sugawara, A.; Ishii, T.; Kato, T. *Angew. Chem.* **2003**, *115*, 5457.
(30) Sukhorukov, G. B.; Volodkin, D. V.; Günther, A. M.; Petrov, A. I.; Shenoy, D. B.; Möhwald, H. *J. Mater. Chem.* **2004**, *14*, 2073.
(31) Ueno, Y.; Futagawa, H.; Takagi, Y.; Ueno, A.; Mizushima, Y. *J. Controlled Release* **2005**, *103*, 93.
(32) Wei, W.; Ma, G. H.; Hu, G.; Yu, D.; Mcleish, T.; Su, Z. G.; Shen, Z. Y. *J. Am. Chem. Soc.* **2008**, *130*, 15808.
(33) De Angelis, F.; Gentile, F.; Mecarini, F.; Das, G.; Moretti, M.; Candeloro, P.; Coluccio, M.; Cojoc, G.; Accardo, A.; Liberale, C. *Nat. Photonics* **2011**, *5*, 682.

dx.doi.org/10.1021/nl301775x | *Nano Lett.* XXXX, XXX, XXX−XXX